Tapered Nanoantennas for Efficient Broadband Unidirectional Emission Enhancement

Isabelle Staude[1,*], Ivan S. Maksymov[1,+], Manuel Decker[1], Andrey E. Miroshnichenko[1], Dragomir N. Neshev[1], Chennupati Jagadish[2], and Yuri S. Kivshar[1]

[1]Nonlinear Physics Centre, Research School of Physics and Engineering,
The Australian National University, Canberra ACT 0200, Australia
Fax: +61-2-6125-8588; email: *ips124@physics.anu.edu.au, +mis124@physics.anu.edu.au
[2]Department of Electronic Materials Engineering, Research School of Physics and Engineering,
The Australian National University, Canberra ACT 0200, Australia

Abstract

We fabricate and characterize tapered nanoantennas for broadband unidirectional emission enhancement. Our numerical simulations predict that this type of nanoantenna reaches an average efficiency of 20% and an average front-to-back ratio of 20 over the entire operation bandwidth of more than 300 nm. Measured transmittance spectra show distinct broad resonances reflecting the nanoantenna's broadband characteristics.

1. Introduction

Plasmonic nanoantennas have become a subject of considerable theoretical and experimental interest [1]. Numerous intriguing potential applications of nanoantennas have been considered including optical and quantum communication, nonlinear optics, sensing, and photovoltaics. Arrayed nanoantennas like Yagi-Uda architectures downscaled to nanometric dimensions are particularly suited for these applications because they offer high directivity and a strong emission enhancement at the same time. However, classical Yagi-Uda nanoantennas are intrinsically narrowband due to the wavelength selectivity of their arrays, creating the need for new antenna concepts able to provide broadband functionality. Here we demonstrate experimentally a new design of tapered Yagi-Uda optical nanoantenna, which exhibits exceptional directionality of emission together with a spectral bandwidth of more than 300 nm.

2. Nanoantenna design

The antenna design results from the concept of tapered plasmonic Yagi-Uda nanoantennas [2]. A schematic view of the considered nanoantenna is shown in Fig. 1(a). The nanoantenna consists of a reflector, a principal feed element, and an array of equally spaced directors. For our calculations we assume these elements to be made of silver and we aim for a principal emitted wavelength of $\lambda_0 = 1550\,\mathrm{nm}$. The design width of all elements is $a = 50\,\mathrm{nm}$ and the spacing between adjacent elements is $w = 30\,\mathrm{nm}$. Compared to classical design principles the center-to-center spacing of adjacent nanoantenna elements is drastically reduced and reaches deep-subwavelength dimensions ($\lambda_0/(w+a) \approx 19$). As such, this tapered antenna is more compact compared to e.g. grating-based antennas [3], which is essential for high-density integration on a photonic chip.

The length of the feed element is $L_f = \lambda_0/4 = 388\mathrm{nm}$, while the reflector element has a length $L_r = 1.25L_f = 446\mathrm{nm}$, hence it is inductively detuned to resonate at wavelengths longer than the resonance wavelength of the feed. The length of the director elements is slowly tapered along the length of the antenna. For a linear taper the length $L_N(\alpha)$ of the N-th director is a function of the tapering angle

ISBN 978-952-67611-2-1

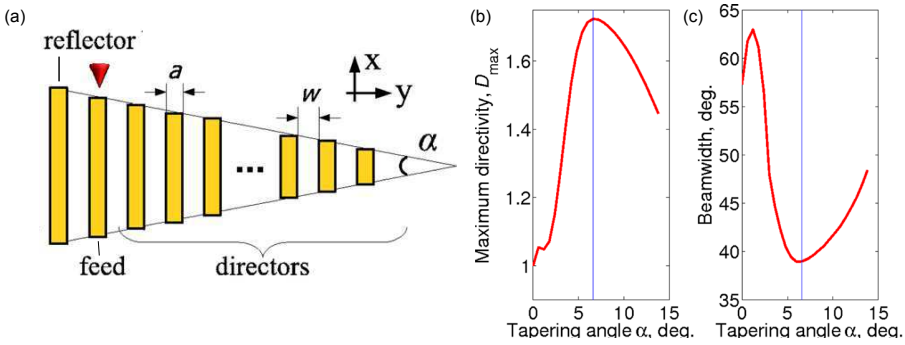

Fig. 1: (a) Schematic view of a tapered nanorod antenna. The arrow denotes the position and polarization of the point-like emitter used for simulations to determine the optimal taper angle. (b) Maximum emission directivity D_{max} and (c) beamwidth of a tapered 42-element Yagi-Uda nanoantenna as a function of α. The straight lines mark $\alpha_{opt} = 6.6°$.

α and is given by to the formula $L_N(\alpha) = L_f - 2N(w+a)\tan(\alpha/2)$, where a is the width of the elements and w is the distance between neighboring antenna elements. First, we study theoretically the angular dependence of the nanoantenna's emission when it is excited via a point-like dipole emitters placed in the hot spot of the feed element. For an optimal taper angle of $\alpha_{opt} = 6.6°$ a pronounced maximum of the directivity [Fig. 1(b)] and a minimum of the beamwidth [Fig. 1(c)] are simultaneously observed [2]. These results are stable against fabrication errors. Additional simulations assuming a director element length variation defined by $L_N/L_{N+1} = 0.99$ furthermore show that this type of nanoantenna indeed offers broadband functionality: Unidirectional emission enhancement is achieved in a *broad operating band* between $1.32\,\mu\mathrm{m}$ and $1.65\,\mu\mathrm{m}$ with average front-to-back ratio between the light emitted into the desired and the opposite direction [3] of $\mathrm{FBR} \approx 20$ and radiation efficiency $\eta \approx 20\%$ [2, 4]. Moreover, at the principal telecom wavelength of $1.55\,\mu\mathrm{m}$ these nanoantennas exhibit theoretical $\mathrm{FBR} = 85$ accompanied by $\eta > 30\%$. We have furthermore checked that it does not impair the performance of the nanoantenna if the silver nanorods are exchanged by gold nanorods, and if a glass substrate is included in these calculations, which merely leads to a spectral shift and to a deflection of the main lobe towards the medium with a higher refractive index.

3. Experimental results

Following our theoretical predictions we have fabricated nanoantennas consisting of 21 nanorods using electron-beam lithography (EBL) followed by evaporation of 50 nm of gold and a lift-off procedure. As substrate we have used glass covered by 7 nm of ITO. In order to allow for assessment of the optical sample quality using far-field spectroscopy we have arranged a large number of nominally identical antennas in a two-dimensional array. The centre-to-centre distance between neighboring antennas is $1\,\mu\mathrm{m}$ in x direction and $2.5\,\mu\mathrm{m}$ in y direction. Furthermore we have rescaled the length of the feed element to 235 nm to shift the antenna's far-field signature into the range of high sensitivity of our characterization setup. The lengths of all other antenna elements are scaled accordingly. A scanning-electron micrograph of such an antenna array with an optimal taper angle of 6.6 degrees is depicted in Fig. 2(a). As a reference we have also fabricated arrays of the same antenna structure but without the reflector and without the taper. These structures allow for an easy theoretical description while posing the same experimental challenges, in particular the very small center-to-center distance of adjacent nanorods of only 80 nm. A high-magnification cutout image of such a reference structure is depicted in Fig. 2(b). Fig. 2(c) shows close-ups of typical individual nanoantennas (i-iii) and reference structures (iv-vii) for different nanorod widths corresponding to different exposure doses during EBL.

For measurement of the resonant frequency of the fabricated structures we have collected perpendicular-incidence linear-optical transmittance spectra using a white-light spectroscopy setup connected to an

ISBN 978-952-67611-2-1

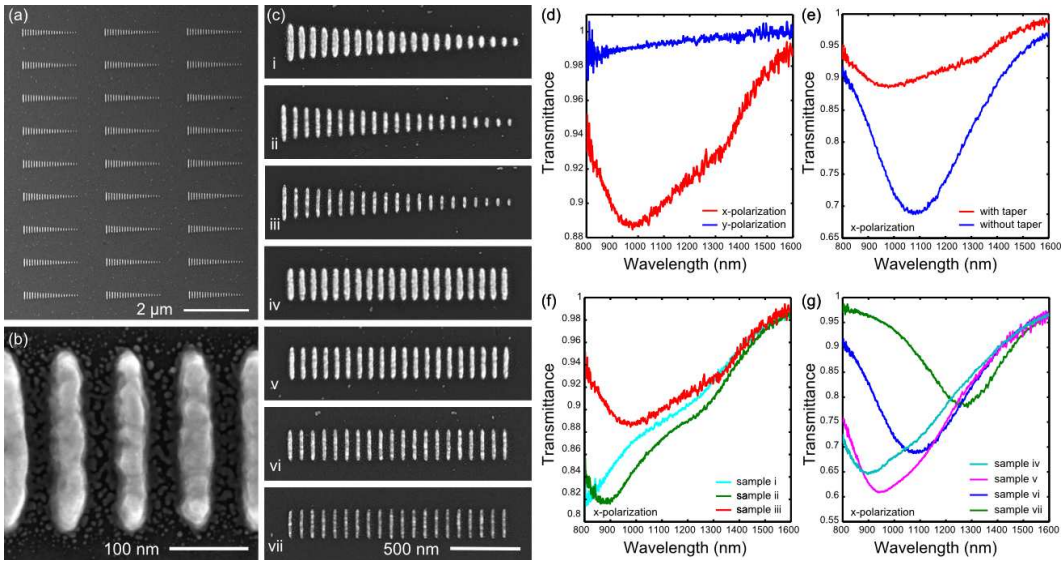

Fig. 2: (a) Fabricated nanoantenna arrays. (b) High-magnification image of a reference structure consisting of gold nanorods of equal length. (c) Close-up electron micrographs of tapered nanoantennas (i-iii) and reference structures (iv-vii) for different EBL exposure doses. (d)-(f) Measured linear-optical transmittance spectra (d) of an array of tapered nanoantennas (sample iii) for the incident light polarized in x and y direction (for definition of the coordinate system see Fig. 1(a)); (e) of an array of tapered nanoantennas compared to an array of reference structures for x-polarized light; (f) of arrays of tapered nanoantennas; and (g) of arrays of reference structures fabricated with different exposure doses.

optical spectrum analyzer. Fig. 2(d) shows transmittance through an array of tapered nanoantennas for the two linear polarizations of the incident light. A broad resonance with a distinct non-Lorentzian shape can clearly be identified for the incident polarization oriented parallel to the long axis of the antenna elements, while transmittance for the orthogonal polarization is close to unity. Note that the overall density of plasmonic structures in the antenna arrays is relatively small, resulting in relatively shallow resonances. In Fig. 2(e) we plot the transmittance for parallel polarization and compare it to corresponding data for the nanoantenna array without the tapers fabricated with the same exposure dose. In the latter case the resonance, which takes on a typical resonance shape, is red-shifted and more pronounced as compared to the tapered case. In order to investigate how inter-element coupling influences the position and the shape of the resonances, we record the transmittance spectra for both tapered and untapered antenna arrays with different nanorod diameters. These results are summarized in Fig. 2(f) and (g), respectively, showing a clear red shift of the resonance position with decreasing nanorod diameter. This shift is not solely governed by the position of the plasmonic resonances of the isolated nanorods, but, as the inter-element spacing is increasing with decreasing nanorod diameter, also influenced by the changed coupling conditions between neighboring nanorods. We have performed CST microwave studio simulations for the control structures revealing that the calculated resonance positions and resonance widths are consistent with experimental results.

In conclusion, we have demonstrated experimentally the fabrication and operation of tapered optical nanoantennas that exhibit strong directional scattering being at the same time broadband over the telecommunication frequency band.

References

[1] V. Giannini, et al., Chem. Rev. **111**, 3888–3912 (2011).
[2] I. S. Maksymov, et al., Appl. Phys. Lett. **99**, 083304 (2011).
[3] A. Baron, et al., Nano Lett. **11**, 4207–4212 (2011).
[4] A. E. Miroshnichenko, et al., Physica Status Solidi RRL **5**, 347–349 (2011).

ISBN 978-952-67611-2-1